Walnut shell supported nanoscale Fe⁰ for the removal of Cu(II) and Ni(II) ions from water

Facui Yang,[1] **Yuanyuan He,**[1] **Shiqi Sun,**[1] **Yue Chang,**[1,2,3] **Fei Zha,**[1,2,3] **Ziqiang Lei**[1,2,3]

[1]College of Chemistry and Chemical Engineering, Northwest Normal University, Lanzhou, Gansu 730070, China
[2]Key Laboratory of Eco-Environment-related Polymer Materials Ministry of Education, Lanzhou, Gansu 730070, China
[3]Key Laboratory of Polymer Material of Gansu Province, Lanzhou, Gansu 730070, China
Correspondence to: Y. Chang (E-mail: cy70@sina.com)

ABSTRACT: The walnut shell supported nanoscale zero-valent iron (walnut-nZVI) was prepared from sodium borohydride, iron(II) chloride tetrahydrate, and walnut shell by liquid phase chemical reduction and characterized by FTIR, TEM, and XRD. The composites were tested as adsorbent for the removal of Cu(II) or Ni(II) ions. The equilibrium data were analyzed by the Langmuir, Freundlich, Dubinin–Radushkevich, which revealed that Langmuir isotherm was more suitable for describing Cu(II) and Ni(II) ions adsorption than the other two isotherm models. The results indicated that the maximum adsorption capacity was higher than some other modified biomass waste adsorbents under the proposed conditions, were 458.7, 327.9 mg g^{-1} for Cu(II) or Ni(II). The adsorption kinetics data indicated that the adsorption fitted well with the pseudo-second-order kinetic model. © 2015 Wiley Periodicals, Inc. J. Appl. Polym. Sci. **2016**, *133*, 43304.

INTRODUCTION

Adsorption has been proved to be one of the most efficient and economical treatment methods for the removal of heavy metals from aqueous media.[1] Activated carbon, zeolite, and fly ash are usually used as adsorbents in adsorption. However, these materials have some deficiencies. The adsorption capacity is small, consumption of adsorbents is large, the regeneration of adsorbents is difficult or cost is too high. So for the preparation of adsorbents, cheap and adsorption capability is large, has become one of researching hotspots currently. A great deal of research indicated that agricultural and forest residues were applied to remove heavy metals from contaminated water at low cost, such as rice husk, corncob, banana peel, and castor leaf.[2–5]

Walnut tree is one of the important economic trees in China. There are considerable numbers of walnut shells produced every year. But a big part of walnut shells are burned down or thrown out, which not only wastes resources but also pollutes the environment. The main components of walnut shell include lignin, cellulose, and hemicelluloses. They have numbers of carboxyl group, carbonyl, and phenolic hydroxyl group. Therefore, walnut shells can be widely used to treat heavy metal polluted waste water because of its better adsorption, iron exchange capacity, and chemical activity. According to reports, walnut shell activated carbon, walnut shell powder, and the modifica-

tion of walnut shell were used to remove heavy metals ions from wastewater, such as Hg(II), Cu(II), Zn(II), Cd(II), Pb(II), and Cr(VI).[6–9] However, two former are high cost or inconvenient post treatment, the latter have slight increase in adsorption capacity for heavy metal ions.

Nanoscale zero-valent iron (nZVI), which has a large surface area and higher surface active, is extensively used in various fields of environment pollution treatment in recent years. For example, the degradation of *p*-nitrophenol in water body, and removal of heavy metals, dyes, nitrates with reducing.[10–13] But powder of nanoscale zero-valent iron nanoparticle is small, easily aggregated, and it also reacts with water or other materials in water, which is difficult to recycle them and reuse. To solve problems mentioned above, zero-valent iron nanoparticles are studied to modify. Supported nano zero-valent iron is one of methods of modification. Supported nano zero-valent iron is not easy to reunite and has good stability. Meanwhile, it is also easy separated from the wastewater to reuse. At present, the materials being used to support nano zero-valent iron are usually molecular sieve silicon, carbon nanotube, and clay.[14–16] However, there are few papers about the research of biomass waste used as carrier. In this study, waste walnut shell produced by Gansu province of China was utilized as the raw material for supporting nano zero-valent iron by liquid phase reducing

method. Using the nano zero-valent iron and functional group of walnut shell to removal Cu(II) and Ni(II) of simulating wastewater. The adsorption behavior of Cu(II) and Ni(II) ions onto walnut shell supported nano zero-valent iron was investigated.

EXPERIMENTAL

Materials

Walnut shell (WS) was crushed into powder, supplied by Gansu province of China. All reagents were analytical graded in this study and included the following: $Cu(NO_3)_2$, $Ni(NO_3)_2$, $NaBH_4$, $FeCl_2 \cdot 4H_2O$, NaOH, HCl, anhydrous alcohol. All aqueous solutions were prepared with redistilled water.

Preparation of Walnut-nZVI

First, 1.83 g of $FeCl_2 \cdot 4H_2O$ was dissolved in 50 mL of 30% (v/v) ethanol solution with stirring and added to a 250-mL three necked flask containing 1.0 g of walnut shell. After the mixture was stirred for 1 h at room temperature under N_2, 100 mL 1.61 mol L^{-1} $NaBH_4$ ethanol solutions was dropped into the mixed solution at a rate of 20–30 drop min^{-1}. Second, the reaction mixtures were thoroughly stirred for 30 min and nitrogen atmosphere was maintained throughout the reaction period. Then the obtained black solid were vacuum filtered and washed with distilled water and subsequently dried at 30°C for 5 h, obtaining walnut-nZVI sample for following use.

Characterization

FT-IR spectra of walnut shell and walnut-nZVI were recorded by using an American Digilab Merlin FTS 3000 FT-IR spectrometer with the KBr pellets in the range of 4000–400 cm^{-1}. XRD analyses of the powered samples were performed using an X-ray power diffractometer (D/Max-2400, Rigaku Japan) with Cu Kα radiation (40 kV, 150 mA). Transmission electron microscopy (TEM) images were captured on a JEOL JEM-2100 electron microscope operated at 500 kV. The concentrations of Cu(II) or Ni(II) were determined by Flame Atomic Adsorption Spectrophotometer (Hitachi Z-2000, Hitachi, Japan). The pH of the zero point charge (pH_{ZPC}) of the walnut-nZVI was followed by a procedure reported earlier.[3] The experiment was carried out in 50 mL conical flasks by adding 0.5 g of walnut-nZVI in 10 mL of CO_2-free water. The flask was sealed with a rubber stopper and stirred continuously by a magnetic stirrer for 48 h at 25°C. Then the solution pH was measured and this value is the pH_{ZPC} of the walnut-nZVI.

Adsorption Studies

Equilibrium batch adsorption studies were carried out with 10.0 mg adsorbent and was added into 100-mL conical flask containing 10 mL of solution with a desired concentration of Cu(II) or Ni(II) ions at room temperature. Appropriate amount of 0.1 mol L^{-1} of HCl or NaOH solutions was used to adjust and control the initial pH of the heavy metals solution. Then the mixture was shaken to reach equilibrium and later magnetic separation filter was used. The final concentration of metal ion was determined in the filtrate by atomic adsorption spectrophotometer. The amount of metal ion adsorbed per unit mass of adsorbent (q_e) was calculated using the following equation:
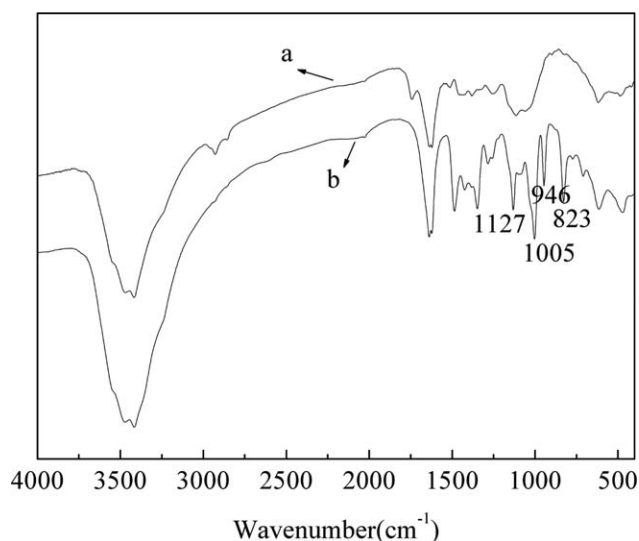

Figure 1. FTIR spectras of walnut shell (a) and walnut-nZVI (b).

$$q_e = (C_0 - C_e) \cdot V / W \qquad (1)$$

Where C_0 and C_e represent initial and equilibrium concentrations of certain heavy metal ion in solution (mg L^{-1}), respectively, V is the volume of solution (L), W is the weight of dry walnut or walnut-nZVI (g).

In the tests of the reusability of walnut-nZVI, 10 mg of walnut-nZVI was added into 10 mL of Cu(II) or Ni(II) solution. After shaking for 1 h at room temperature, the mixture was centrifuged, and then 10.0 mL of fresh Cu(II) or Ni(II) solution were added to the Cu/Ni-loaded walnut-nZVI sample. The process was repeated for five successive trials.

RESULTS

Characterizations of Adsorbents and Adsorption Products

The FTIR spectra of walnut shell (a) and walnut-nZVI (b) were shown in Figure 1. The characteristic bands for walnut shell [Figure 1(a)] were observed at 3440 cm^{-1} (v_{-OH}), 2930 and 2850 cm^{-1} (v_{-CH}), and 1640 cm^{-1} ($v_{-C=O}$). The band in the range of 1000–1130 cm^{-1} was assigned to v_{C-O}/v_{C-O-C}. The characteristic band of walnut shell at 3440 cm^{-1} was obviously increased after reaction [see Figure 1(b)], indicating the presence of massive hydroxyl groups on the surface which was related to the presence of ferric hydroxide (FeOOH) of walnut-nZVI. In addition, the band at 1005 and 946 cm^{-1} which were the bending characteristic bands for hydroxyl groups of ferric hydroxide (FeOOH). The bands at 823 cm^{-1} can be attributed to iron oxides on the surface, as Fe^0 was partially oxidized.[14,17] The intense characteristic band at 1484 and 1350 cm^{-1} were due to ethanol used in preparing the sample. All these variations showed a convincing evidence of the nano zero-valent iron loaded on walnut shell.

TEM images of walnut shell and walnut-nZVI were shown in Figure 2. Walnut shell fibers can be seen in Figure 2(a), which were distributed in chain-like structures. After supporting nano zero-valent iron, it was obvious that there were a large number of nano zero-valent iron particles attached on the surface of the walnut shell fibers and combined together to form a chain
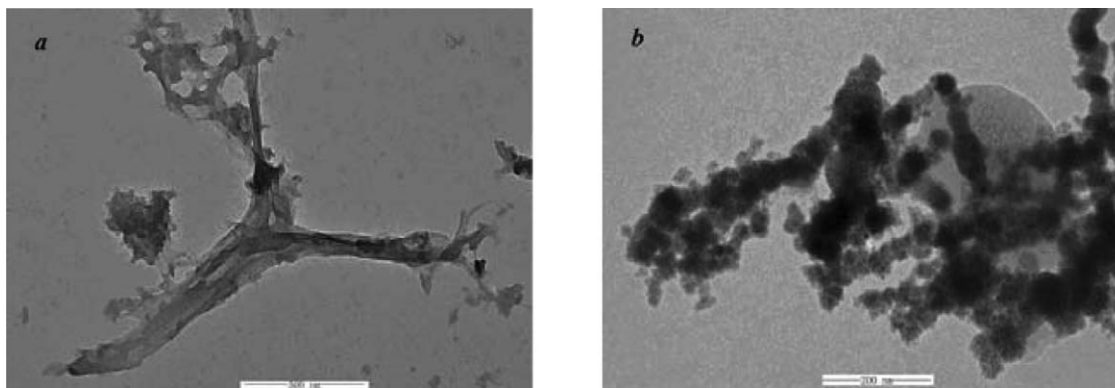
Figure 2. TEM images of walnut shell (a) and walnut-nZVI (b).

structure [Figure 2(b)]. TEM confirmed the walnut shell fibers well dispersed nano zero-valent iron particles.

Figure 3 showed the XRD patterns of walnut shell and walnut-nZVI. For walnut shell sample [Figure 3(a)], the broad peak reveals the existence of an amorphous phase of walnut shell, and the peak was still only one due to the walnut shell mainly consists of cellulose, hemicelluloses, and lignin. Compared to walnut shell, XRD curve of walnut-nZVI appeared many new diffraction peaks: the peaks at 45.3° belonged to diffraction peak of zero-valent (Fe^0), the peaks at 20.2°, 24.6°, 29.9°, 32.5° were observed for γ-Fe_2O_3, the peaks at 16.4°, 30.3°, 39.7°, 41.6°, 46.6°, and 49.5° were observed for γ-FeOOH [Figure 3(b)]. The core-shell structure of iron nanoparticles, the core was ferromagnetic α-Fe with a cubic structure, which was coated with a layer of thin shell oxide γ-FeOOH, it had been recognized as the inherent structure of nano zero-valent iron. γ-FeOOH passive layer was formed during synthesis of nano zero-valent iron in aqueous solution. These results were in agreement with literatures.[18] In addition, part of zero-valent (Fe^0) was partially oxidized to change into γ-Fe_2O_3 when walnut-nZVI was dried.

Effect of Solution pH and Removal Mechanism

The solution pH is an important factor that affects both the speciation of metal ion in solution, and the speciation of the surface of adsorbent in contact with the solution. According to the copper and nickel ions speciation analysis, Cu^{2+} is the predominant ionic species at pH <7.[16] When the solution pH was adjusted from 3.0 to 7.0, the dominant chemical form of Ni in aqueous media was Ni^{2+}.[19] The adsorption experiments were carried out by adjusting the pH (2.0, 3.0, 4.0, 5.0, 6.0) and the initial concentration Cu(II) or Ni(II) ions solution of 200 mg L^{-1} with 10.0 mg of the adsorbent. The effect of the initial pH on walnut-nZVI samples removal for Cu(II) or Ni(II) ions were shown in Figure 4. It can be seen that the adsorption capacity of Cu(II) or Ni(II) ions increased with increasing pH, especially from 2.0 to 3.0. When the pH of solution is 6.0, a complete removal appears to be achieved on both ions. The efficiency of adsorption is dependent on the solution pH, since variation in pH leads to the features of dissociation activity of functional group. It was thought that in low acidic condition it could be attributed to the partial protonation of the active groups which caused repulsion of groups with positive charge and found it hard to donate their electron pairs to coordinate with Cu(II) or Ni(II), thus weakening the complexation
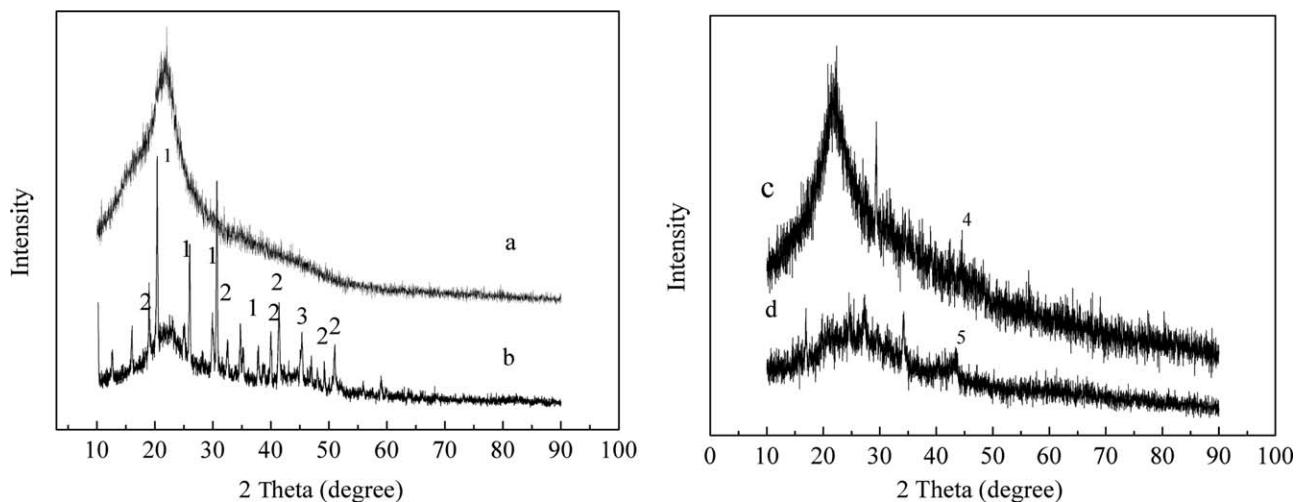

Figure 3. XRD patterns of walnut shell (a), walnut-nZVI (b) (1 = γ-Fe_2O_3, 2 = γ-FeOOH, 3 = Fe^0), walnut-nZVI after adsorption of Cu(II) (4 = Cu^0) (c) and walnut-nZVI after adsorption of Ni(II) (d) (5 = Ni^0).
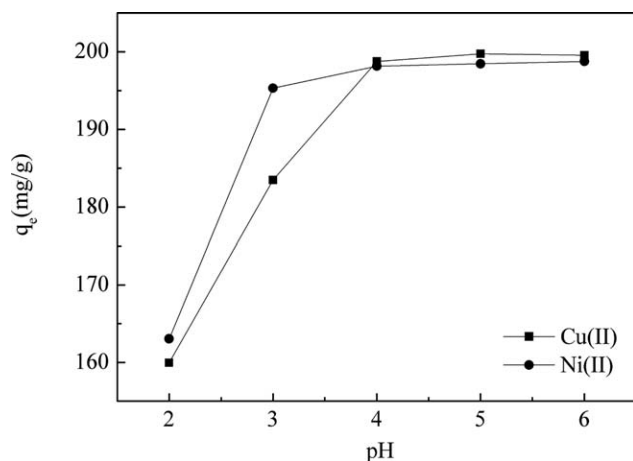
Figure 4. Effect of pH on the adsorption capacity of adsorbent for Cu(II) and Ni(II) (adsorbent dose 10 mg, temperature 293 K).

Figure 6. Effect of connect time on the adsorption capacity of adsorbent for Cu(II) and Ni(II) (adsorbent dose 10 mg, temperature 293 K, pH 5.0).

between them and further decreasing the Cu(II) or Ni(II) adsorption capacity. Furthermore, at low pH, it could be attributed partly to the competition between H^+ and Cu(II) or Ni(II) on the surface sites. With the rising of pH, the hydronium ions reduced and metal ions had competitive advantage to binding more metal ions.

Compared with walnut-nZVI, the experiments were performed using 200 mg L^{-1} of initial concentration of metal ions solutions with the pH values 5.0 and 10.0 mg adsorbent (Figure 5). The adsorption capacities of walnut shell for Cu(II) or Ni(II) ions was 89.0 and 34.4 mg g^{-1}, respectively. But the two metal ions could be removed completely onto walnut-nZVI. The result indicated that the modification strikingly enhanced their adsorption of Cu(II) and Ni(II) ions.

After reaction with the initial concentration of 200 mg L^{-1} Cu(II) or Ni(II) ions, XRD curves [Figure 3(c,d)] appear other specific diffractive peaks of Cu^0 and Ni^0. The high adsorption capacity seemed to be closely related to the mechanism of
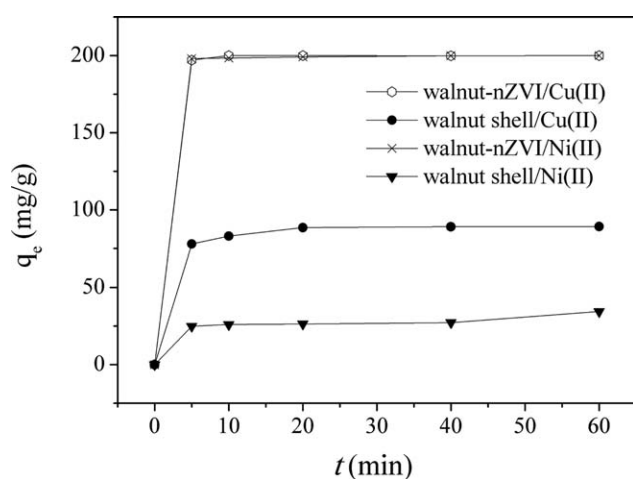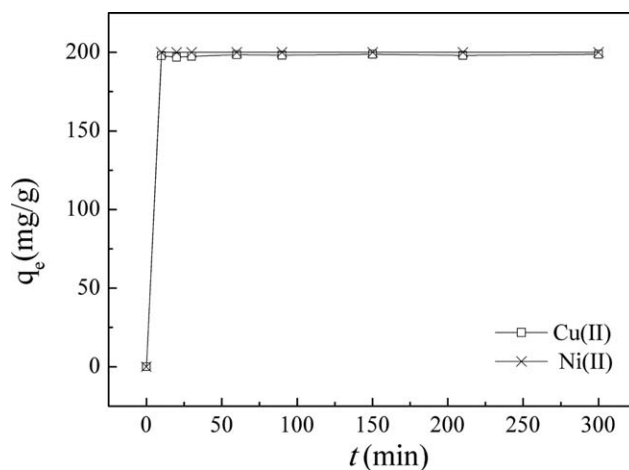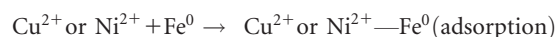

Figure 5. The adsorption capacity of Cu(II) and Ni(II) on walnut shell and walnut-nZVI. The initial Cu(II) or Ni(II) concentration and the content of adsorbent were 200 mg L^{-1} and 1.0 g L^{-1}, respectively. The pH was controlled at 5.0 ± 0.1.

removal, mainly by coordination bond of walnut shell, adsorption, and reduction of Fe^0. The FeOOH, more —OH on the surface was likely the result of the Cu(II) or Ni(II) ions fast adsorption on the surface. It could be deduced that chemical redox reaction occurred during Cu(II) or Ni(II) ions retention.[20]

Cu^{2+} or Ni^{2+} + OH/COOH-walnut shell $\rightarrow$ Cu^{2+} or Ni^{2+}—OH/COOH-walnut shell (coordination complexes)

$$Cu^{2+} \text{ or } Ni^{2+} + Fe^0 \rightarrow Cu^{2+} \text{ or } Ni^{2+}—Fe^0 (\text{adsorption})$$

$$M^{2+} + Fe^0 \rightarrow M^0 + Fe^{2+} (\text{redox}) \ (M^{2+} = Cu^{2+} \text{ or } Ni^{2+})$$

However, there are two reasons that affect the adsorption of metal ions. The initial pH of the solution in the batch tests was 6.0, and the final pH values remained in the range of 7.0–7.5 during the whole adsorption process, and the metal ions formed insoluble hydroxide precipitates simultaneously at pH value >7.0. The adsorption properties of oxide and oxyhydroxide groups on the shell of iron nanoparticles are strongly affected by the solution pH. Therefore, the initial pH of solution was 5.0 since acidic solution that could be dissolved FeOOH layer on the surface of zero-valent iron nanoparticles, but also to remove the efficiency of the metal ions.[21] On the other hand, the pH of the zero point charge (pH_{ZPC}) of walnut-nZVI was determined to be 8.03. As can be seen from Figure 4, the maximum adsorption of Cu(II) and Ni(II) onto walnut-nZVI was at pH 6.0 being much lower than the pH_{ZPC}, revealing the positive charge of the surfaces of walnut-nZVI. Hence, surface complexation in the adsorption of Cu(II) or Ni(II) ions seems to be insignificant, the adsorption process is dominated by redox reaction with walnut-nZVI.

Effect of Contact Time

Nearly 10.0 mg of walnut-nZVI was suspended in 10 mL of the initial concentration Cu(II) or Ni(II) ions solution of 200 mg L^{-1}. The effects of contact time on Cu(II) or Ni(II) removal by the adsorbents were shown in Figure 6. Obviously, the adsorptions of Cu(II) and Ni(II) have similar tendency, the adsorption was rapid in the first stage (0–5 min), the adsorption capacity of

Table I. Kinetic Constants of Cu(II) or Ni(II) Adsorption on Walnut-nZVI at 293 K and Analyzed by the Pseudo-First-Order and Pseudo-Second-Order Models

Adsorbent	$q_{e,exp}$ (mg g^{-1})	Pseudo-first-order			Pseudo-second-order		
		k_1 (min^{-1})	q_e (mg g^{-1})	R^2	k_2 (g (mg min^{-1})$^{-1}$)	q_e (mg g^{-1})	R^2
Cu(II)	199.5	−2.51	0.707	0.186	0.47	200	1
Ni(II)	198.6	4.52E-04	3.332	0.065	0.272	198.8	0.999

Table II. Langmuir, Freundlich, and Dubinin–Radushkevich Isotherm Parameters for the Adsorption of Cu(II) or Ni(II) on Walnut-nZVI

Metal ions	T temp; K	Langmuir				Freundlich			D-R			
		q_m mg g^{-1}	K_L L mg^{-1}	R_L	R^2	K_F L mg^{-1}	$1/n$	R^2	q_{max} mg g^{-1}	β (mol^2 J^{-2})	R^2	E (kJ mol^{-1})
Cu(II)	293	398.4	0.029	0.147	0.944	199.8	0.084	0.572	351.2	1.21E-7	0.812	2.03
	303	458.7	0.057	0.081	0.987	176.4	0.152	0.919	311.8	8.17E-9	0.761	7.82
	313	408.2	0.032	0.135	0.957	212.8	0.080	0.571	305.4	2.24E-5	0.992	0.149
Ni(II)	293	258.4	0.151	0.032	0.999	107.3	0.152	0.894	249.9	1.45E-5	0.959	0.186
	303	271.7	0.080	0.059	0.999	76.68	0.218	0.785	260.1	3.37E-5	0.984	0.122
	313	327.9	0.065	0.007	0.999	72.76	0.263	0.737	308.0	2.58E-5	0.969	0.139

Cu(II) or Ni(II) ions were 197.8, 199.7 mg g^{-1}, respectively. After 10 min, the metal ions could be removed completely in solution. According to numerical results, the initial adsorption behavior occurred on the surface of nZVI and the surface and internal holes of walnut shell, which gave it countless bonding sites. With the extension of adsorption time, adsorption activity sites were decreased that the adsorption tended to equilibrium.

Adsorption Kinetics

The adsorption kinetics Cu(II) or Ni(II) of on walnut-nZVI was analyzed by applying the pseudo-first-order and pseudo-second-order kinetic models[22] to fit the experimental data, expressed respectively as:

$$\ln(q_e - q_t) = \ln q_e - k_1 t \qquad (2)$$

Table III. The Comparison of Maximum Adsorption Capacity of Walnut-nZVI for Cu(II) or Ni(II) with Some Literature Values

Adsorbents	Adsorption capacity (mg g^{-1})		References
	Cu(II)	Ni(II)	
Coconut dregs residue	2.76	5.86	[26]
Walnut sawdust		6.43	[27]
Peanut husk	10.15		[28]
Sulfuric acid modified wheat bran	51.5		[29]
Jujube complex bead	3.64		[30]
Carrot residues	32.74		[31]
Walnut shell-nZVI	458.7	327.9	In this work

$$t/q_t = 1/(k_2 \cdot q_e^2) + 1/q_e \qquad (3)$$

where q_t and q_e (mg g^{-1}) are the amounts of metal ions adsorbed per unit mass of the adsorbent at time t and at equilibrium, k_1 (min^{-1}) is the first order rate constant of adsorption, k_2 (g mg^{-1} min^{-1}) was the rate constant of adsorption equilibrium in the second order reaction.

The kinetic model parameters were obtained from fitting results and presented in Table I. From the relative coefficient R^2, it can be seen that the pseudo-second-order kinetic model fitted the adsorption of Cu(II) or Ni(II) on walnut-nZVI was better than the pseudo-first-order model. It can be obtained that the computed adsorption capacities of metal ions were close to experimental results. According to the assumptions of the pseudo second-order kinetics model, the adsorption way of walnut-nZVI for Cu(II) or Ni(II) included the external liquid film diffusion, surface adsorption, and intra-particle diffusion.

Adsorption Isotherms. The equilibrium sorption experimental data obtained in this study were analyzed using the commonly used Langmuir isotherm and Freundlich and Dubinin-Radushkevich (D-R) models.[23–25]

The Langmuir isotherms model was described by the following equation:

$$c_e/q_e = c_e/q_m + 1/(q_m \cdot K_L) \qquad (4)$$

where c_e is the equilibrium concentration of metal ions remained in the solution (mg L^{-1}); q_e is the amount of metal ions adsorbed on per weight unit of solid after equilibrium (mg g^{-1}); q_m, the maximum adsorption capacity, is the amount of adsorbate at complete monolayer coverage (mg g^{-1}), and K_L (L mg^{-1}) is a constant that relates to the heat of adsorption.
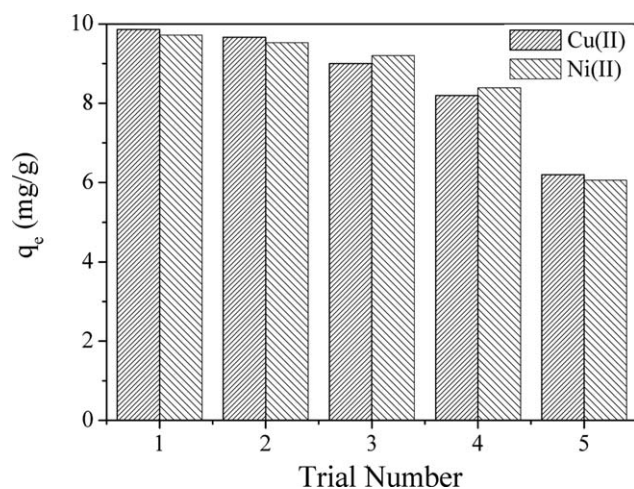
Figure 7. The adsorption capacity of Cu(II) and Ni(II) ions on walnut-nZVI with the number of successive applications of the sorbent sample at the initial concentrations of 10.0 mg L^{-1}.

The Freundlich isotherm model represents properly the adsorption data at low and intermediate concentrations on heterogeneous surfaces, expressed by the equation:

$$n q_e = \ln K_F + (1/n) \ln c_e \tag{5}$$

where K_F and n are Freundlich constants which are related to adsorption capacity and intensity of adsorption. The relative values calculated from the two models were listed in Table II. The adsorption capacities of Cu(II) or Ni(II) were increased with the increasing of temperature. As can be seen from the correlation coefficients R^2, the adsorption process can be better modeled by Langmuir equation. The active sites on their surface were monolayer adsorption for Cu(II) or Ni(II). The highest value of q_{max} obtained for Ni(II) and Cu(II) at 313 K was 327.9 and 458.7 mg g^{-1}, respectively.

The Dubinin–Radushkevich (D-R) isotherm is also used to analyze the experimental isotherm data. Its linearized expression is shown as below:

$$\ln q_e = \ln q_m - \beta \varepsilon^2 \tag{6}$$

where q_e (mg g^{-1}) is the sorbed value of the metal ions at equilibrium concentration, q_m (mg g^{-1}) is the theoretical saturation capacity, β (mol^2 J^{-2}) is a constant related to the sorption energy, ε is the Polanyi potential. The Polanyi potential given as: $\varepsilon = RT \ln(1 + 1/c_e)$, R is the universal gas constant (8.314 J mol^{-1} K^{-1}) and T is the absolute temperature (K). The values of q_m and β can be evaluated from the intercept and slope of the linear plot of lnq_e versus ε. The D-R constant (β) can give the valuable information regarding the mean energy of adsorption[25]: $E = 1/(2\beta)^{-0.5}$

The free energy of adsorption values (E) means that the mean required to transfer 1 mol of ions from bulk solution to the surface of the adsorbent, to explain the adsorption process is a chemical adsorption, ion exchange, or physical adsorption. As can be seen from Table II, physical adsorption was the main factor because the values of E were <8 kJ mol^{-1}. Comparing to other biomass waste adsorbents, the adsorption capacities of

walnut-nZVI for Cu(II) or Ni(II) were the highest (Table III). This study also showed that the walnut-nZVI as adsorbent material had the potential to practical application for Cu(II) or Ni(II) ions. More importantly, the walnut-nZVI is cheap and easy to produce. Besides, the adsorbent is separated from the wastewater.

The experiments of the reusability of walnut-nZVI were conducted to evaluate their removal capability toward Cu(II) or Ni(II). The obtained results for two metal ions were given in Figure 7. As was seen, at the initial concentration of 10.0 mg L^{-1} the walnut-nZVI was very successful in removing the Cu(II) or Ni(II) ions completely after the third cycle of application. Beyond three cycles, a gradual decrease in the adsorption capacity of the walnut-nZVI takes place. The experiments on repetitive loading indicated that walnut-nZVI do not lose their reactivity toward Cu(II) or Ni(II) ions even after three applications in the lower concentrations.

CONCLUSIONS

Walnut-nZVI composite had been prepared and applied to remove Cu(II) and Ni(II) from water, respectively. The adsorption studies have shown that the kinetics of the adsorption of Cu(II) or Ni(II) on walnut-nZVI perfectly followed the pseudo-second-order kinetic model, implying the possibility of chemisorptions. The adsorption isotherms were well fitted by the Langmuir equation. The reusability study revealed that the adsorbents could be efficiently recycled for three times under the lower concentrations conditions. These findings suggested that walnut-nZVI had higher adsorption capacities and faster speed for Cu(II) or Ni(II). Compared with other agricultural and forest residues as biosorbents, it is a kind of new method to the treatment of heavy metal wastewater in applications.

REFERENCES

1. Yang, W.; Ding, P.; Zhou, L.; Yu, J.; Chen, X.; Jiao, F. *Appl. Surf. Sci.* **2013**, *282*, 38.

2. Ajmal, M.; Khan Rao, R. A.; Anwar, S.; Ahmad, J.; Ahmad, R. *Bioresour. Technol.* **2003**, *86*, 147.

3. Leyva-Ramos, R.; Bernal-Jacome, L. A. *Sep. Purif. Technol.* **2005**, *45*, 41.

4. Martins, A. E.; Pereira, M. S.; Jorgetto, A. O.; Martines, M. A. U.; Silva, R. I. V.; Saeki, M. J.; Castro, G. R. *Appl. Surf. Sci.* **2013**, *276*, 24.

5. Bhatnagara, A.; Sillanpää, M. *Chem. Eng. J.* **2010**, *157*, 277.

6. Zabihi, M.; Ahmadpour, A.; Haghighi, A. A. *J. Hazard. Mater.* **2009**, *167*, 230.

7. Nowicki, P.; Pietrzak, R.; Wachowska, H. *Catal. Today* **2010**, *150*, 107.

8. Urkan, A. T.; Pehlivan, E. *Food Chem.* **2012**, *132*, 693.

9. Saadat, S.; Karimi-jashni, A. *Chem. Eng. J.* **2011**, *173*, 743.

10. Tang, L.; Tang, J.; Zeng, G.; Yang, G.; Xie, X.; Zhou, Y.; Pang, Y.; Fang, Y.; Wang, J.; Xiong, W. *Appl. Surf. Sci.* **2015**, *333*, 220.

11. Bhowmick, S.; Chakraborty, S.; Mondal, P.; Renterghem, W. V.; Berghe, S. V.; Roman-Ross, G.; Chatterjee, D.; Iglesias, M. *Chem. Eng. J.* **2014**, *243*, 14.

12. Liu, C.; Li, X.; Ma, B.; Qin, A.; He, C. *Appl. Surf. Sci.* **2014**, *321*, 158.

13. Zhang, Y.; Li, Y.; Li, J.; Hu, L.; Zheng, X. *Chem. Eng. J.* **2011**, *171*, 526.

14. Kim, S. A.; Kannan, S. K.; Lee, K. J.; Park, Y. J.; Shea, P. J.; Lee, W. H.; Kim, H. M.; Oh, B. T. *Chem. Eng. J.* **2013**, *217*, 54.

15. Lee, K. J.; Lee, Y.; Yoon, J. S. K. K.; Parka, S. M.; Oh, B. T. *Environ. Technol.* **2009**, *30*, 1425.

16. Üzüm, C.; Shahwan, T.; Eroğlu, A. E.; Hallamb, K. R.; Scottb, T. B.; Lieberwirth, I. *Appl. Clay Sci.* **2009**, *43*, 172.

17. Ishikawa, T.; Yasukawa, A.; Kandori, K. *Chem. Soc. Faraday Trans.* **1994**, *90*, 2567.

18. Drbohlavova, J.; Hrdy, R.; Adam, V. *Sensors* **2009**, *9*, 2352.

19. Kamari, A.; Mohd Yusoff, S. N.; Abdullah, F.; Putra, W. P. *J. Environ. Chem. Eng.* **2014**, *2*, 1912.

20. Yan, W.; Herzing, A. A.; Kiely, C. J.; Zhang, W. *J. Contam. Hydrol.* **2010**, *118*, 96.

21. Sun, Y. P.; Li, X. Q.; Cao, J.; Wang, H. P. *Adv. Colloid Interface Sci.* **2006**, *120*, 47.

22. Xu, Y. H.; Zhao, D. Y. *Water Res.* **2007**, *41*, 2101.

23. Chen, S. Y.; Zou, Y.; Yan, Z. Y.; Shen, W.; Shi, S.; Zhang, X.; Wang, H. *J. Hazard. Mater.* **2009**, *161*, 1355.

24. Wang, X.; Patil, P. D.; He, C.; Huang, J.; Liu, Y. N. *J. Appl. Polym. Sci.* **2015**, *161*, 41597, DOI: 10.1002/APP.41597.

25. Brdar, M.; Šćiban, M.; Takači, A.; Došenović, T. *Chem. Eng. J.* **2012**, *183*, 108.

26. Taty-costodes, V. C.; Fauduet, H.; Porte, C. *J. Hazard. Mater.* **2003**, *105*, 121.

27. Bulut, Y.; Tez, Z. *Environ. Bull.* **2003**, *12*, 1499.

28. Li, Q.; Zhai, J.; Zhang, W.; Wang, M.; Zhou, J. *J. Hazard. Mater.* **2006**, *141*, 163.

29. Yan, H.; Dai, J.; Yang, Z.; Yang, H.; Cheng, R. *Chem. Eng. J.* **2011**, *174*, 586.

30. Choi, J. W.; Chung, S. G.; Hong, S. W.; Kim, D. J.; Lee, S. H. *Water Air Soil Pollut.* **2012**, *223*, 1837.

31. Nasernejad, B.; Zadeh, T. E.; Pour, B. B.; Bygi, M. E.; Zamani, A. *Process Biochem.* **2005**, *40*, 1319.